



ISSN NO. 2320-5407

Journal homepage: <http://www.journalijar.com>

INTERNATIONAL JOURNAL
OF ADVANCED RESEARCH

RESEARCH ARTICLE

Zygophyllum coccineum L. Extract as green corrosion inhibitor for copper in 1 M HNO₃ Solutions

A.S. Fouda¹, Y.M. Abdallah^{2,*}, G.Y. Elawady¹ and R.M. Ahmed¹

1) Department of Chemistry, Faculty of Science, El-Mansoura University, El-Mansoura-35516, Egypt,

2) Faculty of Oral and Dental Medicine, Delta University for science and Technology, Gamasa, Egypt,

Manuscript Info

Manuscript History:

Received: 15 September 2014

Final Accepted: 15 October 2014

Published Online: November 2014

Key words: Acidic inhibition,
Zygophyllum coccineum L.Extract,
Green inhibitor, SEM.

*Corresponding Author

Y.M.Abdallah

E-mail:

dr.ymostafa80@yahoo.com

Abstract

Zygophyllum coccineum L. Extract (ZCE), was investigated as a green corrosion inhibitor for copper in 1 M HNO₃ solutions using weight loss, potentiodynamic polarization, electrochemical impedance spectroscopy (EIS) and electrochemical frequency modulation (EFM) techniques. Surface morphology was tested using scanning electron microscope (SEM). The effect of the temperature on corrosion behavior with addition of different concentrations was studied in the temperature range of 25-45 °C by weight loss method. Polarization curves reveal that the investigated extract is a mixed type inhibitors. The inhibition efficiency was found to increase with increase in the investigated extract concentration and decrease with raising solution temperature. The adsorption of the inhibitor on copper surface was found to obey the Langmuir's adsorption isotherm. The results obtained from chemical and electrochemical techniques are in good agreement.

Copy Right, IJAR, 2014. All rights reserved

Introduction

Copper is a metal that has a wide range of applications due to its good properties. It is used in electronics, for production of wires, sheets, tubes, and also to form alloys. The use of copper corrosion inhibitors in acid solutions is usually to minimize the corrosion of copper during the acid cleaning and descaling. The possibility of the copper corrosion prevention has attracted many researchers so until now numerous possible inhibitors have been investigated (Khaled, 2009, Kosec *et al.* 2008, Rahmouni *et al.* 2007).

Most well-known acid inhibitors are organic compounds containing nitrogen, sulfur, and oxygen atoms. Among them, organic inhibitors have many advantages such as high inhibition efficiency and easy production (Singh *et al.* 1993, Banerjee *et al.* 1992, Arab *et al.* 1993, Raspini 1993). Organic heterocyclic compounds have been used for the corrosion inhibition of copper (Villamil *et al.* 1999) in different corroding media. Although many of these compounds have high inhibition efficiencies, several have undesirable side effects, even in very small concentrations, due to their toxicity to humans, deleterious environmental effects, and high-cost (Parikh *et al.* 2004).

Plant extract is low-cost and environmental safe, so the main advantages of using plant extracts as corrosion inhibitor are economic and safe environment. Up till now, many plant extracts have been used as effective corrosion inhibitors for copper in acidic media, such as: Zenthoxylum alatum (Chauhan, 2009), Azadirachta Indica (Sangeetha, *et al.* 2011) caffeine (Fernando Silvio de Souza *et al.* 2012) Cannabis (Abd-El-Nabeyet *et al.* 2013). The inhibition performance of plant extract is normally ascribed to the presence of complex organic species, including tannins, alkaloids and nitrogen bases, carbohydrates and proteins as well as hydrolysis products in their composition. These organic compounds usually contain polar functions with nitrogen, sulfur, or oxygen atoms and have triple or conjugated double bonds with aromatic rings in their molecular structures, which are the major adsorption centers.

Zygophyllum coccineum L, is a type genus of flowering plants in Zygophyllaceae family. The eleven species it contains are known generally as White Alratrit, is widely distributed in Mediterranean, The whole plant has great

medicinal importance, as Uses repellent worms, hypotensive , decrease the percentage of sugar in the blood and used as Antipyretic and anti-fever (Gibbons *et al.* 2001).

The present work was designed to study the inhibitory action of *Zygothallum coccineum* L extract for the corrosion of copper in 1 M HNO₃ using chemical and electrochemical techniques. Also, the surface morphology was tested using scanning electron microscope (SEM).

Material and Methods

2.1. Materials and Solutions

Experiments were performed using copper specimens (99.98%) which were mounted in Teflon. An epoxy resin was used to fill the space between Teflon and copper electrode. The auxiliary electrode was a platinum sheet (1 cm²), saturated calomel electrode (SCE) as reference electrode was connected to a conventional electrolytic cell of capacity 100 ml via a bridge with a Luggin capillary, the tip of which was very close to the surface of the working electrode to minimize the IR drop. The aggressive solution used was prepared by dilution of analytical reagent grade 70% HNO₃ with bidistilled water. The stock solution (1000 ppm) of ZCE was used to prepare the desired concentrations by dilution with bidistilled water. The concentration range of ZCE used was 50-500 ppm.

2.2. Preparation of plant extracts

Fresh aerial parts of ZCE sample were crushed to make fine powder. The powdered materials (250 g) were soaked in 500 ml of dichloromethane for 5 days and then subjected to repeated extraction with 5× 50 ml until exhaustion of plant materials. The extracts obtained were then concentrated under reduced pressure using rotary evaporator at temperature below 50°C. The dichloromethane evaporated to give solid extract that was prepared for application as corrosion inhibitor. Chemical studies have demonstrated that the ZCE contain:

Zygothallin (28% in leaves, 0.18% in stems and 0.26% in fruits), Quinovic acid (0.36% in leaves, 0.31% in fruits and 0.47% in stems) and Flavonoids e.g. kaempferol-3- rutinoside (El-Moghazy, 1957, Boulos, 2000).

2.3. Weight loss measurements

Seven parallel copper sheets of 1×1×0.2 cm were abraded with emery paper (grade 320–500–1200) and then washed with bidistilled water and acetone. After accurate weighing, the specimens were immersed in a 250 ml beaker, which contained 100 ml of HNO₃ with and without addition of different concentrations of ZCE. All the aggressive acid solutions were open to air. After 180 minutes, the specimens were taken out, washed, dried, and weighed accurately. The average weight loss of seven parallel copper sheets could be obtained. The inhibition efficiency (IE %) and the degree of surface coverage, θ of ZCE for the corrosion of copper were calculated as follows (Mu *et al.* 1996),

$$IE\% = \theta \times 100 = \left[1 - \frac{W}{W^0}\right] \times 100 \quad (1)$$

where W^0 and W are the values of the average weight loss without and with addition of the inhibitor, respectively.

2.4. Electrochemical measurements

All the measurements were done in solutions open to atmosphere under unstirred conditions. All potential values were reported versus SCE. Prior to each experiment, the electrode was treated as before. Tafel polarization curves were obtained by changing the electrode potential automatically from (-0.8 to 1 V vs. SCE) at open circuit potential with a scan rate of 1 mVs⁻¹. Stern-Geary method (Parr *et al.* 1978), used for the determination of corrosion current is performed by extrapolation of anodic and cathodic Tafel lines to a point which gives (log i_{corr}) and the corresponding corrosion potential (E_{corr}) for inhibitor free acid and for each concentration of inhibitor. Then (i_{corr}) was used for calculation of inhibition efficiency (IE %) and surface coverage (θ) as in equation 2:

$$IE\% = \theta \times 100 = \left[1 - \frac{i_{corr(inh)}}{i_{corr(free)}}\right] \times 100 \quad (2)$$

where $i_{corr(free)}$ and $i_{corr(inh)}$ are the corrosion current densities in the absence and presence of inhibitor, respectively . Impedance measurements were carried out in frequency range (2×10^4 Hz to 8×10^{-2} Hz) with amplitude of 10 mV peak-to-peak using ac signals at open circuit potential. The experimental impedance was analyzed and interpreted based on the equivalent circuit. The main parameters deduced from the analysis of Nyquist diagram are the charge transfer resistance R_{ct} (diameter of high-frequency loop) and the double layer capacity C_{dl} . The inhibition efficiencies and the surface coverage (θ) obtained from the impedance measurements are calculated from equation 3:

$$IE\% = \Theta \times 100 = \left[1 - \left(\frac{R_{ct}^{\circ}}{R_{ct}} \right) \right] \times 100 \quad (3)$$

where R_{ct}° and R_{ct} are the charge transfer resistance in the absence and presence of inhibitor, respectively. Electrochemical frequency modulation (EFM) was carried out using two frequencies 2 and 5 Hz. The base frequency was 0.1 Hz, so the waveform repeats after 1 s. The higher frequency must be at least two times the lower one. The higher frequency must also be sufficiently slow that the charging of the double layer does not contribute to the current response. Often, 10 Hz is a reasonable limit. The Intermodulation spectra contain current responses assigned for harmonical and intermodulation current peaks. The large peaks were used to calculate the corrosion current density (i_{corr}), the Tafel slopes (β_a and β_c) and the causality factors CF-2&CF-3 (Bosch *et al.* 2001). The electrode potential was allowed to stabilize 30 min before starting the measurements. All the experiments were conducted at 25°C.

All electrochemical measurements were performed using Gamry Instrument (PCI4/750) Potentiostat/Galvanostat/ZRA. This includes a Gamry framework system based on the ESA 400. Gamry applications include DC105 software for potentiodynamic polarization, EIS300 software for electrochemical impedance spectroscopy, and EFM140 software for electrochemical frequency modulation measurements via computer for collecting data. Echem Analyst 6.03 software was used for plotting, graphing, and fitting data. To test the reliability and reproducibility of the measurements, duplicate experiments, which performed in each case at the same conditions.

2.5. Surface morphology

For morphological study, surface features (1 cm x 1 cm x 0.2cm) of copper were examined before and after exposure to 1 M HNO_3 solutions for 12 hours with and without ZCE. JEOL JSM-5500 scanning electron microscope was used for this investigation.

Result and Discussion

3.1. Weight loss measurements

Weight loss measurements were carried out for copper in 1 M HNO_3 in the absence and presence of different concentrations of ZCE and are shown in Figure (1). The inhibition efficiency (IE %) values calculated are listed in Tables 1& 2. From these tables, it is noted that the IE% increases steadily with increasing the concentration of ZCE and decrease with raising the temperature from 25-45°C. The inhibition efficiency (IE %) and surface coverage (θ) were calculated by equation (1).

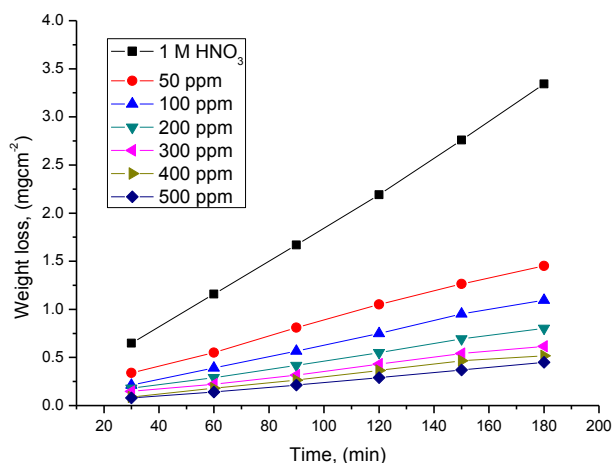


Figure1: Weight loss-time curves for the corrosion of copper in 1 M HNO_3 in the absence and presence of different concentrations of ZCE at 25°C

Table 1: Corrosion rate (C.R.) and inhibition efficiency data obtained from weight loss measurements for copper in 1 M HNO₃ solutions without and with various concentrations of ZCE at 25°C

Conc., ppm	Weight loss, Mg cm ⁻²	C.R., mg cm ⁻² min ⁻¹	θ	%IE
1 M HNO ₃	3.44	0.027	---	---
50	1.10	0.019	0.680	68.0
100	0.80	0.017	0.767	76.7
200	0.50	0.006	0.855	85.5
300	0.47	0.004	0.863	86.3
400	0.43	0.003	0.875	87.5
500	0.31	0.001	0.91	91.0

Table 2: Data of weight loss measurements for copper in 1 M HNO₃ solution in the absence and presence of different concentrations of ZCE at 25–45°C

Conc., ppm	Temp., °C	C.R., mgcm ⁻² min ⁻¹	θ	IE%
50	25	0.019	0.680	68.0
	30	0.065	0.620	62.0
	35	0.083	0.536	53.6
	40	0.120	0.473	47.3
	45	0.237	0.410	41.0
100	25	0.017	0.767	76.7
	30	0.022	0.638	63.8
	35	0.042	0.548	54.8
	40	0.053	0.490	49.0
	45	0.062	0.453	45.3
200	25	0.006	0.855	85.5
	30	0.017	0.793	79.3
	35	0.027	0.685	68.5
	40	0.038	0.543	54.3
	45	0.050	0.496	49.6
300	25	0.004	0.863	86.3
	30	0.016	0.809	80.9
	35	0.023	0.743	74.3
	40	0.035	0.694	69.4
	45	0.060	0.547	54.7
400	25	0.003	0.875	87.5
	30	0.015	0.832	83.2
	35	0.021	0.773	77.3
	40	0.028	0.753	75.3
	45	0.036	0.621	62.1
500	25	0.001	0.910	91.0
	30	0.011	0.848	84.8
	35	0.017	0.805	80.5
	40	0.023	0.782	78.2
	45	0.037	0.653	65.3

The observed inhibition action of the ZCE could be attributed to the adsorption of its components on copper surface. The formed layer, of the adsorbed molecules, isolates the metal surface from the aggressive medium which limits the dissolution of the latter by blocking of their corrosion sites and hence decreasing the corrosion rate, with increasing efficiency as their concentrations increase (Zhang *et al.* 2009).

3.2. Polarization measurements

Figure 2 shows potentiodynamic polarization curves recorded for copper in 1 M HNO₃ solutions in the absence and presence of various concentrations of ZCE at 25°C.

Lee and Nobe (Lee *et al.* 1986) reported the occurrence of a current peak between the apparent-Tafel and limiting-current regions during potential sweep experiments. The presence of ZCE shifts both anodic and cathodic branches to the lower values of corrosion current densities and thus causes a remarkable decrease in the corrosion rate. The parameters derived from the polarization curves in Figure 2 are given in Table 3. In 1 M HNO₃ solution, the presence of ZCE causes a remarkable decrease in the corrosion rate i.e., shifts both anodic and cathodic curves to lower current densities. In other words, both cathodic and anodic reactions of copper electrode are retarded by ZCE in 1 M HNO₃ solution. The Tafel slopes of β_a and β_c at 25°C do not change remarkably upon addition of ZCE, which indicates that the presence of ZCE does not change the mechanism of hydrogen evolution and the metal dissolution process. Generally, an inhibitor can be classified as cathodic type if the shift of corrosion potential in the presence of the inhibitor is more than 85 mV with respect to that in the absence of the inhibitor (Tao *et al.* 2009, Ferreira *et al.* 2004). In the presence of ZCE, E_{corr} shifts to less negative but this shift is very small (about 20-30 mV), which indicates that ZCE can be arranged as mixed type inhibitor. Since $\beta_c > \beta_a$, ZCE is classified as mixed type inhibitor but the cathode is more polarized than the anode when an external current was applied.

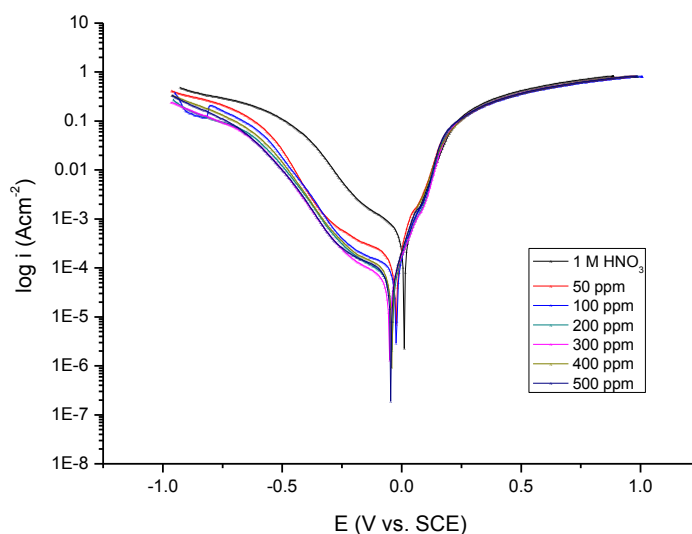


Figure 2: Potentiodynamic polarization curves for the corrosion of copper in 1 M HNO₃ solution without and with various concentrations of ZCE at 25°C.

Table 3: Effect of concentration of ZCE on the electrochemical parameters calculated using potentiodynamic polarization technique for the corrosion of copper in 1 M HNO₃ at 25°C.

Concentration, ppm	i_{corr} , $\mu\text{A cm}^{-2}$	$-E_{\text{corr}}$, mV vs. SCE	β_a , mVdec ⁻¹	β_c , mVdec ⁻¹	CR, mm y ⁻¹	θ	η %
1 M HNO ₃	363.0	10.7	86	207	179.30	--	--
50	124.0	20.4	77	287	61.22	0.658	65.8
100	120.0	24.6	77	234	59.39	0.669	66.9
200	56.5	22.9	73	224	27.86	0.844	84.4
300	54.1	40.0	69	224	26.68	0.851	85.1
400	42.7	42.9	76	214	21.06	0.882	88.2
500	36.3	50.0	80	212	17.94	0.900	90.0

3.3. Electrochemical impedance spectroscopy (EIS)

EIS is well-established and powerful technique in the study of corrosion. Surface properties, electrode kinetics and mechanistic information can be obtained from impedance diagrams (Silverman *et al.* 1988, Lorenz *et al.* 1981, Macdonald *et al.* 1982, Mansfeld 1981, Gabrielli 1982) Figure 3 and Figure 4 show the Nyquist and Bode plots respectively, obtained at open-circuit potential both in the absence and presence of increasing concentrations of ZCE at 25°C. The increase in the size of the capacitive loop with the addition of ZCE extract shows that a barrier gradually forms on the copper surface. From the Bode plots (Fig.4), the total impedance increases with inhibitor concentration ($\log Z$ vs. $\log f$). But ($\log f$ vs. phase) the continuous increase in the phase angle shift, obviously correlating with the increase of inhibitor adsorbed on Cu surface. The Nyquist plots do not yield perfect semicircles as expected from the theory of EIS. The deviation from ideal semicircle was generally attributed to the frequency dispersion (El Achouri *et al.* 2001) as well as to the in homogeneities of the copper surface.

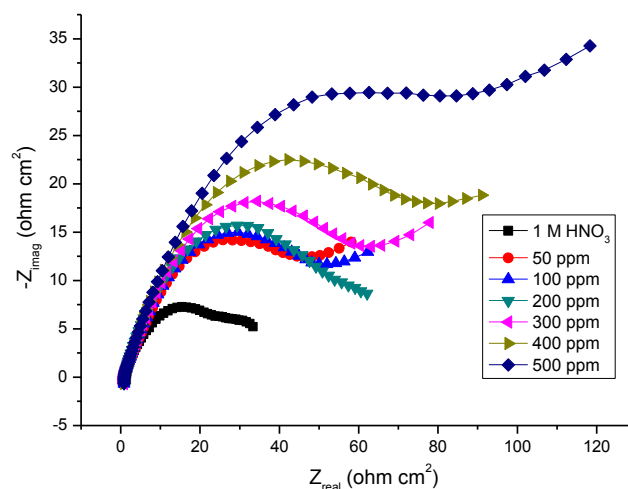


Figure 3. Nyquist plots recorded for copper in 1 M HNO₃ without and with various concentrations of ZCE at 25°C

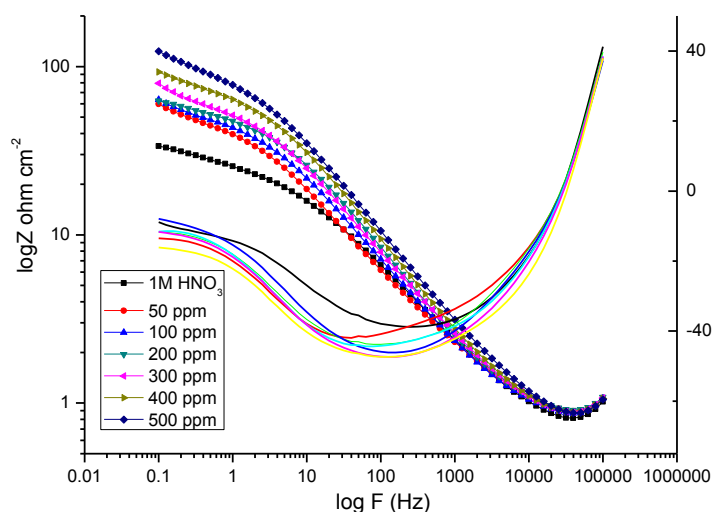


Figure 4. Bode plots recorded for copper in 1 M HNO₃ without and with various concentrations of ZCE at 25°C

EIS spectra of the investigated extract were analyzed using the equivalent circuit in Figure 5, which represents a single charge transfer reaction and fits well with our experimental results. The constant phase element, CPE, is introduced in the circuit instead of a pure double layer capacitor to give a more accurate fit (Macdonald *et al.* 1987). The double layer capacitances, C_{dl} , for a circuit including a CPE parameter (Y_0 and n) were calculated from the following equation (Tao *et al.* 2009):

$$C_{dl} = Y_0 (\omega_{max})^{n-1} \quad (4)$$

where Y_0 is the magnitude of the CPE, $\omega_{max} = 2\pi f_{max}$, f_{max} is the frequency at which the imaginary component of the impedance is maximal and the factor n is an adjustable parameter that usually lies between 0.5 and 1.0. After analyzing the shape of the Nyquist plots, it is concluded that the curves approximated by a single capacitive semicircles, showing that the corrosion process was mainly charged-transfer controlled (Mertens *et al.* 1997, Trabanelli *et al.* 2005). The general shape of the curves is very similar for all samples (in presence or in absence of ZCE at different immersion times) indicating that no change in the corrosion mechanism (Trowsdate *et al.* 1996). From the impedance data (Table 4), we conclude that the value of R_{ct} increases with increase in concentration of the ZCE and this indicates an increase in % IE.

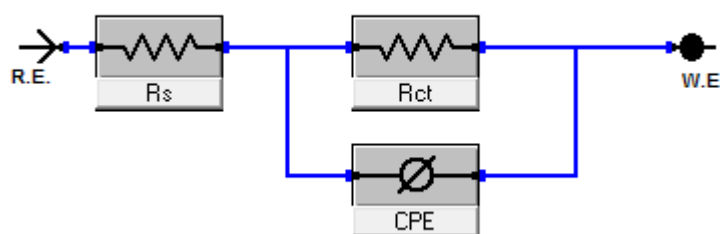


Figure 5. Electrical equivalent circuit used to fit the impedance data

Table 4. Electrochemical kinetic parameters obtained from EIS technique for copper in 1M HNO_3 solution containing various concentrations of ZCE at 25°C.

Conc., ppm,	R_{ct} , $\Omega \text{ cm}^2$	C_{dl} , $\mu\text{F cm}^{-2}$	θ	IE %
1 M HNO_3	20.84	874.8	---	---
50	60.46	814.5	0.655	65.5
100	69.65	783.5	0.701	70.1
200	73.56	732.3	0.717	71.7
300	75.45	700.9	0.724	72.4
400	87.19	657.8	0.761	76.1
500	119.8	632.7	0.826	82.6

The presence of ZCE enhances the value of R_{ct} in acidic solution. Values of double layer capacitance are also brought down to the maximum extent in the presence of ZCE and the decrease in the values of CPE follows the order similar to that obtained for i_{corr} in this study. The decrease in CPE/C_{dl} results from a decrease in local dielectric constant and/or an increase in the thickness of the double layer, suggesting that ZCE extract inhibit the copper corrosion by adsorption at metal/acid (Reis *et al.* 2006, Lagrenee *et al.* 2002, McCafferty *et al.* 1972). The inhibition efficiency is calculated from the charge-transfer resistance data as shown in equation 3 (Ma *et al.* 2002)

3.4. Electrochemical frequency modulation (EFM)

EFM is a nondestructive corrosion measurement technique that can directly determine the corrosion current value without prior knowledge of Tafel slopes, and with only a small polarizing signal. These advantages of EFM technique make it an ideal candidate for online corrosion monitoring (Kus *et al.* 2006). The great strength of the EFM is the causality factors which serve as an internal check on the validity of EFM measurement. The causality

factors CF-2 and CF-3 are calculated from the frequency spectrum of the current responses. Figure 6 show the frequency spectrum of the current response of pure copper in 1 M HNO₃ solution, contains not only the input frequencies, but also contains frequency components which are the sum, difference, and multiples of the two input frequencies. The EFM intermodulation spectrums of Cu in 1 M HNO₃ solution containing (50ppm- 500ppm) of the ZCE extract at 25 °C is shown in Figure 6. The harmonic and intermodulation peaks are clearly visible and are much larger than the background noise. The two large peaks, with amplitude of about 200 μA, are the response to the 40 and 100 mHz (2 and 5 Hz) excitation frequencies. It is important to note that between the peaks there is nearly no current response (<100 mA). The experimental EFM data were treated using two different models: complete diffusion control of the cathodic reaction and the “activation” model. For the latter, a set of three non-linear equations had been solved, assuming that the corrosion potential does not change due to the polarization of the working electrode (Caigman *et al.* 2000). The larger peaks were used to calculate the corrosion current density (i_{corr}), the Tafel slopes (β_c and β_a) and the causality factors (CF-2 and CF-3). These electrochemical parameters were simultaneously determined by Gamry EFM140 software, and listed in Table 5 indicating that this extract inhibit the corrosion of copper in 1 M HNO₃ through adsorption. The causality factors obtained under different experimental conditions are approximately equal to the theoretical values (2 and 3) indicating that the measured data are verified and of good quality (Abdel-Rehim *et al.* 2006). The inhibition efficiencies IE_{EFM} % increase by increasing the studied extract concentrations and was calculated as follows:

$$IE \%_{EFM} = \left(1 - \frac{i_{corr}}{i_{corr}^0} \right) \times 100 \quad (5)$$

where i_{corr}^0 and i_{corr} are corrosion current densities in the absence and presence of ZCE extract, respectively.

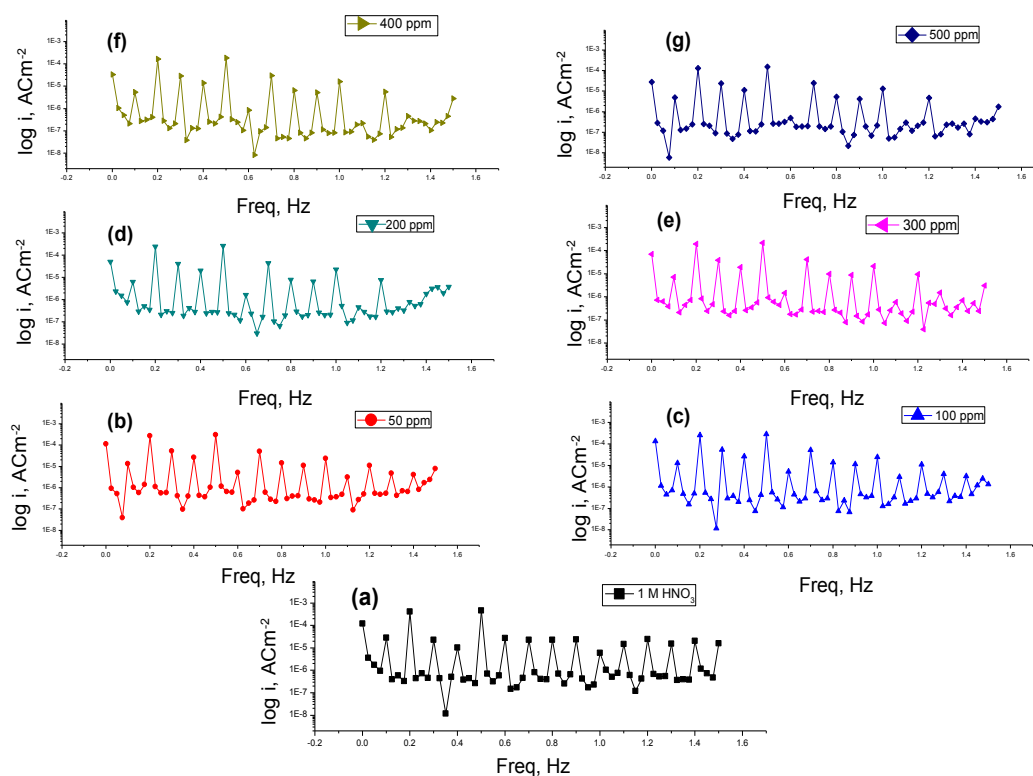


Figure 6 (a-g): Intermodulation spectrums for the corrosion of copper in 1 M HNO₃ without and with various concentrations of ZCE at 25°C

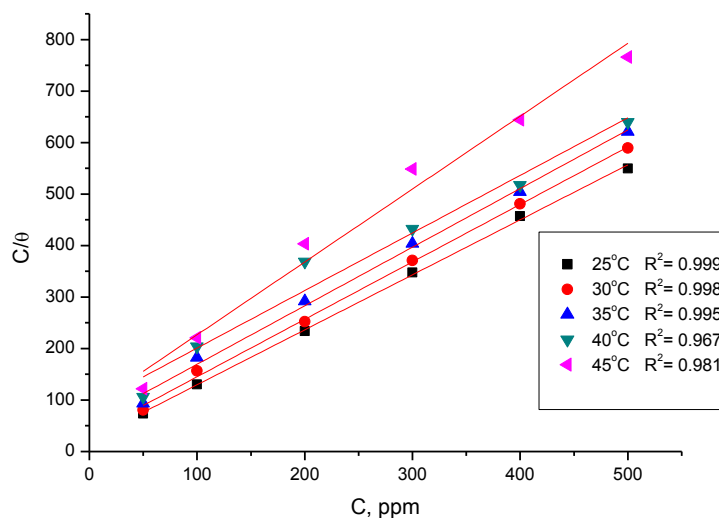
Table 5: Electrochemical kinetic parameters obtained by EFM technique for Cu in 1 M HNO₃ solutions containing various concentrations of ZCE at 25 °C.

Conc., ppm	i_{corr} , μAcm^{-2}	β_a , mV dec^{-1}	β_c , mV dec^{-1}	C.R. mpy	CF-2	CF-3	θ	IE%
1 M HNO ₃	319.6	44.800	52	158	1.76	2.80	---	---
50	183.6	47.730	102	140	1.91	2.92	0.426	42.6
100	167.6	46.650	107	132	2.07	3.10	0.476	47.6
200	134.8	49.700	110	125	1.93	2.92	0.578	57.8
300	105.2	48.280	114	106	2.00	3.24	0.671	67.1
400	63.3	56.250	117	98	1.97	3.10	0.802	80.2
500	38.7	54.520	129	83	2.00	3.13	0.879	87.9

3.5. Adsorption Isotherm

The mode and interaction degree between an inhibitor and a metallic surface have been widely studied with the application of adsorption isotherms. The adsorption of an organic molecule occurs because the interaction energy between an inhibitor and a metallic surface is higher than that between water molecules and metallic surface (Bockris *et al.* 1964, Saleh *et al.* 2006). To obtain the adsorption isotherms, the degree of surface coverage (θ) obtained from weight loss method was determined as a function of inhibitor concentration. The values of θ were then plotted to fit the most suitable model of adsorption (Narvez *et al.* 2005). Attempts were made to fit experimental data to various isotherms including Frumkin, Langmuir, Temkin, Freundlich, isotherms. By far the results were best fitted by Langmuir adsorption isotherm as seen in Figure 7 (Li *et al.* 2009):

$$\frac{C}{\theta} = \frac{1}{K} + C \quad (6)$$

**Figure 7:** Langmuir adsorption plots for copper in 1 M HNO₃ containing various concentrations of ZCE at 25°C

3.6. Kinetic-thermodynamic corrosion parameters

Weight loss method was carried out at different temperature (25 °C–45 °C) in the presence of different concentration of ZCE. It has been found that the corrosion rate increases with the increase in temperature for ZCE (Table 2). The corrosion rate of copper in the absence of ZCE increased steeply from 25 to 45 °C whereas; in the presence of ZCE the corrosion rate decreased slowly. The inhibition efficiency was found to decrease with temperature. The corrosion parameter in the absence and presence of extract in the temperature range 25–45 °C has been summarized in Table 2. The apparent activation energy (E_a^*) for dissolution of copper in 1M HNO₃ was calculated from the slope of plots by using Arrhenius equation:

$$\log k = \frac{-E_a^*}{2.303 R T} + \log A \quad (7)$$

where k is rate of corrosion, E_a^* is the apparent activation energy is the universal gas constant, T is absolute temperature and A is the Arrhenius pre-exponential factor.

By plotting $\log k$ against $1/T$ the values of activation energy (E_a^*) has been calculated ($E_a^* = (\text{slope}) 2.303 \times R$) (Figure 8). Activation energy for the reaction of copper in 1M HNO_3 increases in the presence of extract (Table 6). This increasing in activation energy E_a^* indicates the formation of energy barrier which. However, the extent of the rate increment in the inhibited solution is higher than that in the free acid solution. Therefore, the inhibition efficiency of the ZCE decreases markedly with increasing temperature. This result supports the idea that the adsorption of extract components on the copper surface may be physical in nature. Thus, as the temperature increases the number of adsorbed molecules decreases leading to decrease in the inhibition efficiency. The obtained results suggest that ZCE inhibits the corrosion reaction by increasing its activation energy. This could be done by adsorption on the copper surface making a barrier for mass and charge transfer. Moreover, the relatively low value of activation energy in presence of ZCE suggests a physical adsorption process.

The values of change of entropy (ΔS^*) and change of enthalpy (ΔH^*) can be calculated by using the formula:

$$k = \left(\frac{RT}{Nh}\right) \exp\left(\frac{\Delta S^*}{R}\right) \exp\left(\frac{\Delta H^*}{RT}\right) \quad (8)$$

where k is rate of corrosion, h is Planck's constant, N is Avogadro number, ΔS^* is the entropy of activation, and ΔH^* is the enthalpy of activation. A plot of $\log(k/T)$ vs. $1/T$ (Figure 9) should give a straight line, with a slope of $(\Delta H^*/2.303R)$ and an intercept of $[\log(R/Nh) + \Delta S^*/2.303R]$, from which the values of ΔS^* and ΔH^* can be calculated (Table 6). The negative value of ΔS^* for the inhibitor indicates that activated complex in the rate determining step represents an association rather than a dissociation step, meaning that a decrease in disorder takes place during the course of transition from reactant to the activated complex (Saliyan *et al.* 2007) The negative sign of ΔH^* indicates that the adsorption of inhibitor molecules is an exothermic process. Generally, exothermic process signifies either physisorption, chemisorption's or a combination of both.

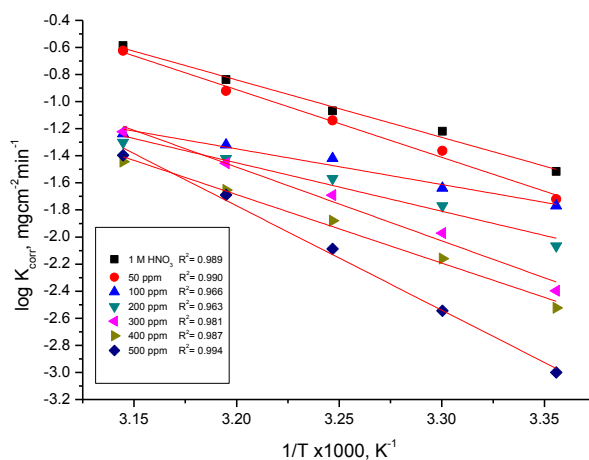


Figure 8: $\log k$ (corrosion rate) – $1/T$ curves for copper in 1 M HNO_3 in the absence and presence of different concentrations of ZCE

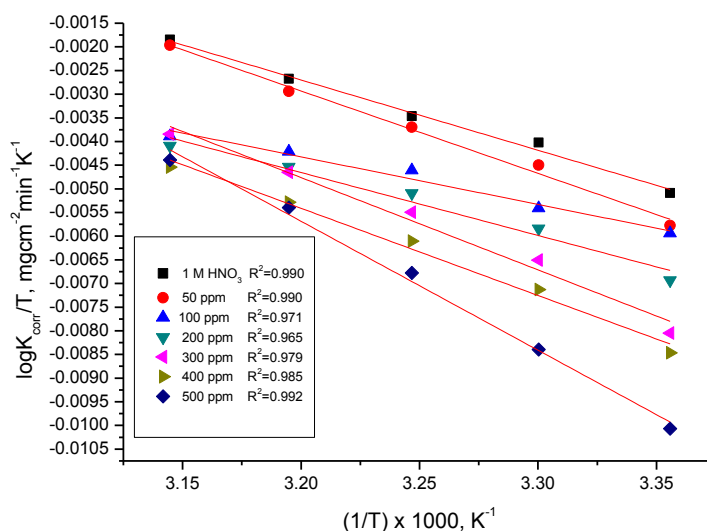


Figure 9: $\log k_{\text{corr}}/T - 1/T$ curves for copper in 1 M HNO_3 in the absence and presence of different concentrations of ZCE.

Table 6: Activation parameters for dissolution of copper in the absence and presence of different concentrations of ZCE in 1 M HNO_3 in the range of 25-45°C.

Conc. ppm	E_a^* , kJ mol^{-1}	ΔH^* , kJ mol^{-1}	$-\Delta S^*$, $\text{J mol}^{-1}\text{K}^{-1}$
1.0 M HNO_3	50.41	83.63	196.71
50	68.49	110.57	196.56
100	81.24	123.37	197.04
200	95.63	144.74	196.85
300	96.85	153.06	196.47
400	104.30	162.12	196.55
500	147.66	226.55	196.01

3.7. Surface analysis by SEM

Figure 10 shows an SEM photograph recorded for copper samples Polished (A) and exposed for 12 h in 1M HNO_3 solution without (B) and with 500 ppm of ZCE at 25°C. A photograph of the polished copper surface before immersion in 1 M HNO_3 solution is shown in Figure 10a. The photograph shows the surface was smooth and without pits. The SEM micrographs of the corroded copper in the presence of 1 M HNO_3 solution are shown in Figure 10b. The faceting seen in this figure was a result of pits formed due to the exposure of copper to the acid. The influence of the inhibitor addition 500 ppm on the copper in 1 M HNO_3 solution is shown in Figure 10c. The morphology in Figure 10c shows a rough surface, characteristic of uniform corrosion of copper in acid, as previously reported (Li *et al.* 2005), that corrosion does not occur in presence of inhibitor and hence corrosion was inhibited strongly when the inhibitor was present in the nitric acid, and the surface layer is very rough. In contrast, in the presence of 500 ppm of ZCE, there is much less damage on the copper surface, which further confirms the inhibition action. Also, there is an adsorbed film adsorbed on copper surface (Figure 10c). In accordance, it might be concluded that the adsorption film can efficiently inhibit the corrosion of copper.

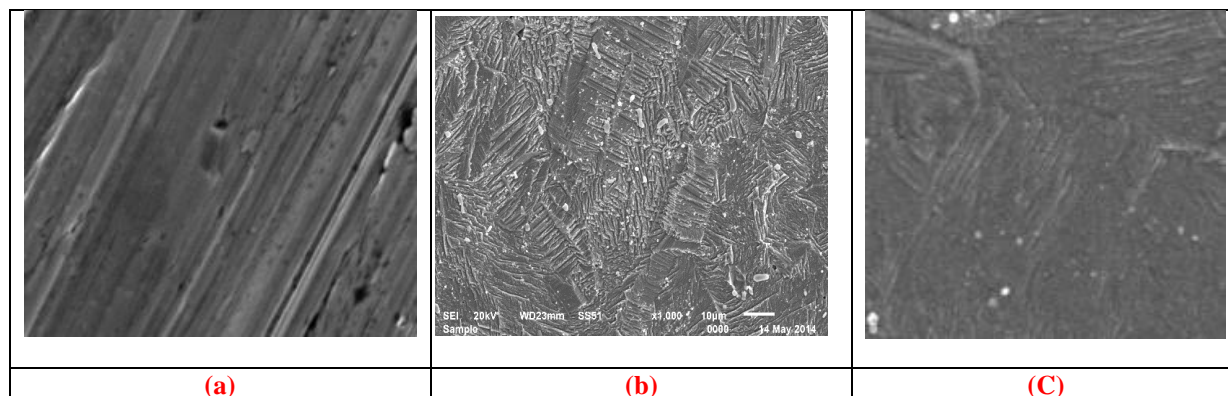


Figure 10: SEM micrographs of copper surface (a) before of immersion in 1 M HNO₃, (b) after 12 h of immersion in 1 M HNO₃ and (c) after 12 h of immersion in 1 M HNO₃ + 500 ppm of ZCE at 25°C

3.8. Mechanism of the corrosion inhibition

Most of organic inhibitors contain at least one polar group with an atom of nitrogen, oxygen, sulphur or in some cases selenium and phosphorus. The inhibiting properties of many compounds are determined by the electron density at the reaction center (Anand *et al.* 1965).

With increase in electron density in the center, the chemisorption between the inhibitor and the metal are strengthened (Cook *et al.* 1951, Bordeaux *et al.* 1957). The plant extract ZCE is composed of numerous naturally occurring organic compounds. Accordingly, the inhibitive action of ZCE could be attributed to the adsorption of its components on the copper surface. The main phytochemical constituents of ZCE are Zygophyllin (28% in leaves, 0.18% in stems and 0.26% in fruits), Quinovic acid (0.36% in leaves, 0.31% in fruits and 0.47% in stems) and Flavonoids e.g. kaempferol-3-rutinoside. Most of these phytochemicals are organic compounds that have center for π -electron and presence of hetero atoms such as oxygen and nitrogen; hence, the adsorption of the inhibitor on the copper surface is enhanced by their presence (Ebenso *et al.* 2008) reported that Quinovic acid and flavonoids are major constituents of plant that enhance the inhibition potentials of plant extracts. Therefore, the inhibition efficiency of methanol extracts of ZCE is due to the formation of multi-molecular layer of adsorption between copper surface and some of these phytochemicals. Results of the present study have shown that ZCE extract inhibits the acid induced corrosion of copper by virtue of adsorption of its components onto the metal surface. The inhibition process is a function of the metal, inhibitor concentration, and temperature as well as inhibitor adsorption abilities, which is so much dependent on the number of adsorption sites. The mode of adsorption (physisorption) observed could be attributed to the fact that ZCE contains many different chemical compounds, which some can be adsorbed physically. This observation may derive the fact that adsorbed organic molecules can influence the behavior of electrochemical reactions involved in corrosion processes in several ways. The action of organic inhibitors depends on the type of interactions between the substance and the metallic surface. The interactions can bring about a change either in electrochemical mechanism or in the surface available for the processes (Singh *et al.* 2010).

Conclusions

From the overall experimental results the following conclusions can be deduced:

1. The ZCE shows good performance as corrosion inhibitor in 1 M HNO₃.
2. The results obtained from weight loss showed that the inhibiting action increases with the ZCE concentration and decreases with the increasing in temperature.
3. Double layer capacitances decrease with respect to blank solution when the plant extract is added. This fact confirms the adsorption of plant extract molecules on the copper surface.
4. The ZCE inhibits the corrosion by getting adsorbed on the metal surface following Langmuir adsorption isotherm.
5. The inhibition efficiencies determined by weight loss, potentiodynamic polarization and EIS techniques are in reasonably good agreement.

References

Abd-El-Nabey B. A., Abdel-Gaber A. M., El. Said Ali M., Khamis E., El-Housseiny S.(2013), Inhibitive Action of Cannabis Plant Extract on the Corrosion of Copper in 0.5 M H₂SO₄. *J. Electrochem. Sci.*, 8: 5851-5865.

Abdel-Rehim S. S., Khaled K. F., Abd-Elshafi N. S.(2006), Electrochemical frequency modulation as a new technique for monitoring corrosion inhibition of iron in acid media by new thiourea derivative. *Electrochim. Acta*, 51: 3269-3277.

Anand R. R., Hurd R. M., Hackerman N.(1965), Adsorption of Monomeric and Polymeric Amino Corrosion Inhibitors on Steel. *J. Electrochem. Soc.* 112:138-144.

Arab S. T., Noor E. A. (1993), Inhibition of Acid Corrosion of Steel by Some S-Alkylisothiuronium Iodides. *Corrosion*, 49: 122-129.

Banerjee G., Malhotra S. N. (1992), Contribution to Adsorption of Aromatic Amines on Mild Steel Surface from HCl Solutions by Impedance, UV, and Raman Spectroscopy. *Corrosion*, 48: 10-15.

Bockris J. O., Swinkels D. A. J. (1964), Adsorption of n-Decylamine on Solid Metal Electrodes. *J. Electrochem. Soc.*, 111: 736-743.

Bosch R. W., Hubrecht J., Bogaerts W. F., Syrett B. C. (2001), Electrochemical Frequency Modulation: A New Electrochemical Technique for Online Corrosion Monitoring. *Corrosion*, 57: 60-70.

Bordeaux J. J. and Hackerman N. (1957), ADSORPTION FROM SOLUTION OF STEARIC ACID ON IRON - EFFECT ON ELECTRODE POTENTIAL. *J. Phys. Chem.* 61: 1323-1327.

Boulos, L. (2000). "Flora of Egypt", volume two, pp. 24, printed by Al Hadara Publishing, Cairo, Egypt.

Caignan G. A., Metcalf S. K., Holt E. M. (2000), X-ray structure of [(μ-H)Os₃(CO)₁₀(μ-1,8-η²-C₉H₆N)]. *J. Chem. Cryst.*, 30: 415-422.

Chauhan J. S. (2009). *Asian Journal of Chemistry*, 21: 1975-1978.

Cook E. L., Hackerman N. (1951), Adsorption of polar organic compounds on steel. *J. Phys. colloid Chem.* 55: 549-557.

Ebenso E. E., Eddy N. O., Odiongenyi A. O. (2008), Corrosion inhibitive properties and adsorption behaviour of ethanol extract of Piper guinensis as a green corrosion inhibitor for mild steel in H₂SO₄. *African J. Pure. Appl. Chem.* 2: 107-115.

El Achouri M., Kertit S., Gouttaya H. M., Nciri B., Bensouda Y., Perez L., Infante M. R., Elkacemi K. (2001), Corrosion inhibition of iron in 1 M HCl by some gemini surfactants in the series of alkanediyl- α,ω -bis-(dimethyl tetradecyl ammonium bromide). *Prog. Org. Coat.*, 43: 267-273.

El-Moghazy, M.A. (1957). "A comparative study of the common Egyptian Zygophyllum species". Ph.D. thesis, Faculty of Pharmacy, Cairo University.

Fernando Sílvia de Souza, Cristiano Giacomelli, Reinaldo Simões Gonçalves, Almir Spinelli. (2012), Adsorption behavior of caffeine as a green corrosion inhibitor for copper. *Materials Science and Engineering*, 32: 2436-2444.

Ferreira E. S., Giacomelli C., Giacomelli F. C., Spinelli A. (2004), Evaluation of the inhibitor effect of l-ascorbic acid on the corrosion of mild steel. *Mater. Chem. Phys.* 83: 129-134.

Gabrielli C., (1980), Identification of Electrochemical processes by Frequency Response Analysis, Solarton Instrumentation Group. *corros. sci.* 21:121-129.

Gibbons S., Oriowo M. A., 2001. Antihypertensive effect of an aqueous extract of *Zygodophyllumcoccineum* L. in rats. *Phytother Res. Aug*; 15(5):452-455.

Khaled K. F. (2009), Experimental and atomistic simulation studies of corrosioninhibition of copper by a new benzotriazole derivative in acid medium. *Electrochim. Acta*, 54: 4345-4352.

Kosec T., Merl D. K., Milošev I. (2008), Impedance and XPS study of benzotriazole films formed on copper, copper–zinc alloys and zinc in chloride solution. *Corros. Sci.*, 50: 1987-1997.

Kus E., Mansfeld F. (2006), An evaluation of the electrochemical frequency modulation (EFM) technique. *Corros. Sci.*, 48: 965-979.

Lagrene M., Mernari B., Bouanis M., Traisnel M., Bentiss F. (2002), Study of the mechanism and inhibiting efficiency of 3,5-bis(4-methylthiophenyl)-4H-1,2,4-triazole on mild steel corrosion in acidic media. *Corros. Sci.*, 44: 573-588.

Lee H. P. andNobe K. (1986), Kinetics and Mechanisms of Cu Electrodisolution in Chloride Media. *J. Electrochem. Soc.* 133: 2035- 2043.

Li Y., Zhao P., Liang Q., Hou B. (2005), Berberine as a natural source inhibitor for mild steel in 1 M H₂SO₄. *Appl. Surf. Sci.*, 252: 1245-1253.

Li X. H., Deng S. D., Fu H. (2009), 3-Hydroxybenzoic acid as AISI 316L stainless steel corrosion inhibitor in a H₂SO₄–HF–H₂O₂ pickling solution. *Corros. Sci.*, 51: 1344-1355.

Lorenz W. J. and Mansfeld F. (1981), Determination of corrosion rates by electrochemical DC and AC methods. *Corros.Sci.*, 21: 647-672.

Macdonald J. R. andJohanson W. B. (1987), In: J.R. Macdonald (Ed.), *Theory in Impedance Spectroscopy*, John Wiley& Sons, New York.

Ma H., Chen S., Niu L., Zhao S., Li S., Li D. (2002), Inhibition of copper corrosion by several Schiff bases in aerated halide solutions. *J. Appl. Electrochem.*, 32: 65.72.

Macdonald D. D. andMckubre M. C. (1981), Impedance measurements in Electrochemical systems,” *Modern Aspects of Electrochemistry*, J.O’M. Bockris, B.E. Conway, R.E. White, Eds., Vol. 14, Plenum Press, New York, New York, P 61, 1982.

Mansfeld F. (1981), Recording and Analysis of AC Impedance Data for Corrosion Studies. *Corrosion*, 37: 301-307.

McCafferty E. andHackerman N. (1972), Double Layer Capacitance of Iron and Corrosion Inhibition with Polymethylene Diamines. *J. Electrochem. Soc.*, 119: 146-154.

Mertens S. F., Xhoffer C., Decooman B. C., Temmerman E. (1997), Short-Term Deterioration of Polymer-Coated 55% Al-Zn — Part 1: Behavior of Thin Polymer Films. *Corrosion*, 53: 381-388.

Mu G. N., Zhao T. P., Liu M., Gu T. (1996), Effect of Metallic Cations on Corrosion Inhibition of an Anionic Surfactant for Mild Steel. *Corrosion*, 52: 853-856.

Narvez L., Cano E., Bastidas D. M. (2005), 3-Hydroxybenzoic acid as AISI 316L stainless steel corrosion inhibitor in a H₂SO₄–HF–H₂O₂ pickling solution. *J. Appl. Electrochem.*, 35: 499-506.

Parikh K. S. and Joshi K. J. (2004), Natural compound onion (*Allium Cepa*), Garlic (*Allium Sativum*) and bitter gourd (*MemordicaCharantia*) as corrosion inhibitors for mildsteel in hydrochloric acid. *Trans. SAEST*, 39: 29-35.

Parr R. G., Donnelly R. A., Levy M., Palke W. E. (1978), Electronegativity- the density functional viewpoint. *J. Chem. Phys.*, 68: 3801-3807.

Rahmouni K., Hajjaji N., Keddami M., Srhiri A., Takenouti H. (2007), The inhibiting effect of 3-methyl 1,2,4-triazole 5-thione on corrosion of copper in 3% NaCl in presence of sulphide. *Electrochim. Acta*, 52: 7519-7528.

Raspini I. A. (1993), Influence of Sodium Salts of Organic Acids as Additives on Localized Corrosion of Aluminum and Its Alloys. *Corrosion*, 49: 821-828.

Reis F. M., de Melo H. G., Costa I. (2006), EIS investigation on Al 5052 alloy surface preparation for self-assembling monolayer. *J. Electrochem. Acta*, 51: 1780-1788.

Saliyan V. R. and Adhikari A. V. (2008), Inhibition of corrosion of mild steel in acid media by N'-benzylidene-3-(quinolin-4-ylthio)propanohydrazide. *Bull. Mater. Saleh M M, Atia A A, 2006. Effect of structure of the ionic head of cationic surfactant on its inhibition of acid corrosion of mild steel. J. Appl. Electrochem.*, 36: 899-905.

Sangeetha T. V. and Fredimoses M. (2011), Green corrosion inhibitors-An Overview. *E-Journal of Chemistry*, 8: (S1), S1-S6.

Silverman D. C. and Carrico J. E. (1988), Electrochemical Impedance Technique — a Practical Tool for Corrosion Prediction. *Corrosion*, 44: 280.287.

Singh D. N. and Dey A. K. (1993), Synergistic Effects of Inorganic and Organic Cations on Inhibitive Performance of Propargyl Alcohol on Steel Dissolution in Boiling Hydrochloric Acid Solution. *Corrosion*, 49: 594-600.

Singh A. K. and Quraishi M. A. (2010), Inhibitive effect of diethylcarbamazine on the corrosion of mild steel in hydrochloric acid. *Corros. Sci.* 52: 1529-1535.

Tao Z. H., Zhang S. T., Li W. H., Hou B. R. (2009), Corrosion inhibition of mild steel in acidic solution by some oxo-triazole derivatives. *Corros. Sci.* 51: 2588-2595.

Trabanelli G., Montecelli C., Grassi V., Frignani A. (2005), Electrochemical study on inhibitors of rebar corrosion in carbonated concrete. *J. Cem. Concr. Res.*, 35: 1804-1813.

Trowsdate A. J., Noble B., Haris S. J., Gibbins I. S. R., Thomson G. E., Wood G. C. (1996), The influence of silicon carbide reinforcement on the pitting behaviour of aluminium. *Corros. Sci.*, 38: 177-191.

Villamil R. F. V., Corio P., Rubim J. C., Siliva Agostinho M. L. (1999), *J. Electroanal. Chem.*, 472:112-118.

Zhang D. Q., Cai Q. R., He X. M., Gao L. X., Kim G. S. (2009), Corrosion inhibition and adsorption behavior of methionine on copper in HCl and synergistic effect of zinc ions. *Mater. Chem. Phys.* 114: 612-617.